Complexation of Cu(II) Ions with the Lowest Generation Poly(amido-amine)-OH Dendrimers: A Molecular Simulation Study

Francisco Tarazona-Vasquez and Perla B. Balbuena*

Department of Chemical Engineering, Texas A&M University, College Station, Texas 77843

Received: March 21, 2005; In Final Form: April 29, 2005

Classical molecular dynamics simulations and density functional theory calculations are performed to obtain insights about the attachment of the copper(II) ion to the lowest generation poly(amido-amine) dendrimer, G0-OH, in aqueous solutions. Various initial configurations of the ion relative to the dendrimer sites are tested and it is concluded that both the solvent as well as—in a lesser degree for low generation dendrimers—the folding of the dendrimer branch play an important role in copper(II) ion complexation. The presence of solvent and branch folding retain the ion close to the atomic binding sites consisting mainly of amide oxygen as well as hydroxyl oxygen but also tertiary amine nitrogen. A discussion of currently available experimental results in Cu(II) complexation in larger generation dendrimers is provided.

1. Introduction

Dendrimers are envisioned as promising materials in many areas of science and technology with applications spanning design of drug delivery systems, light harvesting, electronic devices, and catalysis.[1−5] Poly(amido-amine) (PAMAM) dendrimers have proven successful template agents for several ions, metal atoms, and clusters, including Pt, Pd, Au, Ag, and Cu.[6−11] As ion complexation precedes the formation of embedded metallic nanoclusters, a clear understanding of ion complexation and that of the influence of the factors that affect the complexation process—such as pH, counterion, ligand exchange, and charge transfer—are needed. Due to their own peculiarities each ionic complexation requires individual study; this fact hampers the understanding of currently known systems and the search for new precursor−dendrimer systems for metal nanoparticle synthesis.

Interest in the understanding of complexation of one of the simplest ion−dendrimer systems, namely Cu(II)−PAMAM, is revealed by a number of experimental works directed toward its characterization such as EPR, EXAFS, UV−vis, and AAS[12−16] For instance, the extent of binding of Cu(II) to dendrimers was calculated by mass balance of Cu(II) content in two aqueous solutions, using atomic absorption spectroscopy (AAS),[13] and found to be a pH-dependent process. However, despite many attempts to elucidate the identity of the atoms constituting the first coordination shell of Cu(II) when it coordinates to PAMAM dendrimers in aqueous solutions, the issue is still in debate. Currently proposed coordination sites include all types of nitrogen[12,14,16,17] in $-NH_2$ terminated dendrimers and carboxylate groups in −COO terminated dendrimers.[18] It has been shown that $-NH_2$ terminal groups can be counted as the main complexation sites for Cu(II)[16] in aqueous solutions of $-NH_2$ dendrimers whereas a less important role has been suggested for interior tertiary amines[14,16] and amide N.[17] The presence of water—mainly in axial sites—has been inferred in a few studies[14,16] from comparisons to similar Cu(II) complexes, although such comparisons hardly support ruling out coordination to amide oxygen.[14,17]

Most of the previous work focused on large generation of $-NH_2$ terminated dendrimers, so the information about ion complexation in −OH terminated PAMAM dendrimers is scarce, especially in low generation dendrimers where we are not aware of any related study, perhaps due to difficulties in obtaining and analyzing experimental data. In this context, we expect that our work can help to identify the atoms in the first coordination shell of Cu(II) in the lowest generation dendrimer solutions, a picture that might provide some insights for interpreting experimental results obtained in larger generation dendrimers. We do not intend to extrapolate the results of this work to larger dendrimers; thus, no scaling of Cu(II) loading with generation, size, or molecular weight is being suggested. However, we do expect that some of the patterns observed in the G0-Cu(II) complexes may be found in the outer pockets of larger dendrimers where eventually the ions will be hosted before their entrance into the inner dendrimer voids. We report a systematic investigation of the interactions of Cu(II) with PAMAM−G0-OH dendrimers in aqueous solutions modeled with explicit solvent by means of classical molecular dynamics (MD) and the interactions of Cu(II) with dendrimer fragments studied with density functional theory (DFT).

2. Computational Methodology

Realistic atomistic simulations with explicit solvent pose tremendous computational challenges because large simulation boxes with vast amounts of explicit solvent would be required to reproduce bulk concentrations normally used in experimental studies[14,16,17,19] (e.g., a G4-NH_2 concentration of 2×10^{-5} M would require more than one million water molecules which becomes prohibitive given the current status of computer software/hardware). Therefore, our simulation box is a cube whose edge length is designed to represent a highly concentrated solution of G0-OH, 0.01 M, which corresponds to 0.01 and 0.02 M concentrations of Cu(II) for simulated ion−dendrimer loading ratios of 1:1 and 2:1, respectively. Consequently the edge of our simulation cube is 54.962 Å—the estimated diameter of G0-OH is 15 Å.[20] Then as the most concentrated solution we seek to represent is only slightly higher in Cu(II) than that used in a recent study with larger generation dendrimers,[14] we expect that

* Address correspondence to this author. E-mail: balbuena@tamu.edu.

10.1021/jp051469p CCC: $30.25 © 2005 American Chemical Society
Published on Web 06/02/2005

our simulations can account for the solvent effect in realistic systems. Explicit water SPC/E[21] is used along with chloride anions playing the role of counterions to ensure electroneutrality.

The total potential energy function for MD includes bonded and nonbonded terms. The first terms comprise bond stretching, bond angle bending, and dihedral torsion whose mathematical expressions, equilibrium distances, and force constants are taken from the DREIDING force field[22] whereas long-range Coulombic and short-range Lennard Jones (LJ) potentials represent the nonbonded terms.

Partial charges for G0-OH are obtained from a single point calculation with the B3LYP functional (hybrid HF-DFT) over the optimized structure obtained with Hartree−Fock and the basis set 6-31g(d); except for slight differences the Mulliken[23−25] charge distribution is almost identical with the previously reported one.[26] Cu(II) and Cl^- are modeled as point charges of +2 and −1, respectively.

The energy and length parameters for the LJ potential for atoms other than Cu(II), water O, and H are taken from the DREIDING force field.[22] Parametrization for Cu(II) is explained in section 2.3, whereas the SPC/E potential, a rigid model, based on a LJ sphere centered in the O atom, with the two hydrogens making an HOH angle of 109.47° and with point charges such that the polarizability of water is reproduced[21] is used for this molecule. SPC/E was selected based on its ability to describe properly the liquid state, the coexistence curve, and critical properties of water. Besides that, it is also computationally inexpensive. All cross-interaction parameters are determined by the Lorentz−Berthelot mixing rules. Water polarization effects are effectively included in the SPC/E water model, as mentioned above, but they are not accounted for either the dendrimer or the Cu(II) models.

As explained in the following section, to provide an adequate initial configuration to the system, some of the MD simulations are preceded by vacuum molecular mechanics (MM) minimizations of the dendrimer/ion complex, as implemented in Gaussian03.[27] In the chosen MM procedure, the atomic charges are calculated with a charge equilibration algorithm[28] by using parameters of the universal force field (UFF).[29] Since the UFF does not have short-range LJ parameters for Cu(II), they are approximated with those of Cu(I); this is not a major approximation because the configurations obtained from MM are only used to initialize the full-solvent MD simulations where appropriate parameters are used for each of the atoms including Cu(II) as discussed later.

To complement our MD simulations, and since a complete description of the interactions between ion, dendrimer, and water is not possible to address with QM calculations due to the system size, we use a simplified model to carry out DFT calculations for the dendrimer: a 38-atom fragment consisting of two dendrimer branches growing from one of the two tertiary amine N atoms in the ethylene−diamine (EDA) core. Gaussian03[27] is used for the DFT calculations and the functional B3LYP along with basis sets 6-31g(d) for light atoms and LANL2DZ[30] with pseudopotentials for Cu(II), respectively.

2.1. Models for MD and DFT Simulations. Simulations are performed for five different MD initial configurations: three of them containing a single Cu(II) ion and two others containing two cations; the simulation setups of each case are described below. Each of these initial configurations includes the G0-OH dendrimer in its lowest energy conformer found in a previous work[26] unless otherwise specified: one or two hexahydrated Cu(II) complexes and the corresponding amount of hydrated Cl^- complexes. In all cases the G0-OH molecule is centered in the simulation box. The initial locations of dendrimer and hexahydrated ion were selected either randomly or via a molecular mechanics minimization. In the first case, it was found that after a few MD steps, the relative locations of dendrimer and hydrated ion were similarly independent of their initial random placements. The initial configurations are qualitatively shown in Chart 1.

CHART 1: Choices of Initial Configurations Other than Random Are Explained by This Diagram[a]

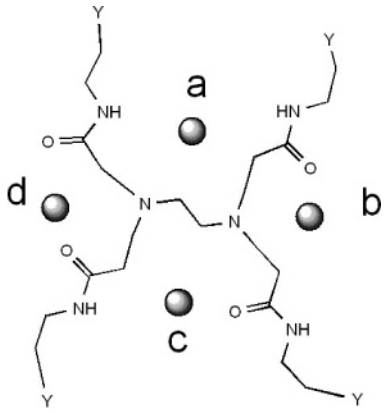

[a] Single ion configurations result from placing the ion either in position b (equivalent to d) or in position a (equivalent to c) and the two-ion configurations are obtained by placing the ions in positions b and d. We did not attempt a configuration with ions in positions a and c as we do not believe such a configuration would be stable (the first ion in either position a or c may coordinate to the core N and therefore the second ion (to be placed in either c or a) might not be able to coordinate to those same atom sites). Note: The purpose of this chart is only to illustrate the criteria used to select initial configurations able to be optimized with MM methods. Y: functional or surface group (in this work −OH).

a. Monoionic Cu(II)-G0 Complexes. Configuration A1: In these simulations, one hexahydrated Cu(II) is added *randomly* to a box containing a G0 dendrimer in its center, and MD simulations are carried out for about 1 ns. Then, after *random* addition of two hydrated Cl^- anions in the voids surrounding the box-centered G0 molecule, additional MD simulations are run for another nanosecond.

Water is added in two steps. First, about 1000 water SPC/E molecules are added to the system and additional simulations are run for 200 ps. The second step involves filling the simulation box with water molecules until approximately liquid water density—it is implicitly assumed that our simulated solution is diluted enough to have a density like pure liquid water—and simulations continue during 600 ps. This last simulation is referred to below as a *full-solvent* simulation.

Configuration A2: In these simulations, one Cu(II) ion and its closest three water molecules are removed from the MM converged configuration calculated for Configuration B2 (vide infra) to become the initial configuration. As a result, Cu(II) is initially *coordinated to two amide O, one core N, and three water O atoms, where no folding branches are present yet*. After 1 ns of MD two hydrated Cl^- are *randomly* added and one additional nanosecond of MD is run. Finally water is added in two steps as in Configuration A1. The MM convergence criteria (in atomic units) are 0.00045 for the maximum force, 0.0003 for the RMS force, 0.0018 for the maximum displacement, and 0.0012 for the RMS displacement, which are the default settings in Gaussian 03[27]

Configuration A3: In these simulations, one Cu(II) is placed *close to two amide O atoms facing toward the two tertiary amine N (atom type NC) atoms of the EDA core* resembling a

configuration used in our Cu(II)-G0 fragment ab initio study.[31] Three water molecules are then added in initial locations estimated with the help of a visualization program and a MM minimization (vide supra) is performed. The procedure continues with 1 ns of MD on the converged MM configuration and one additional nanosecond after *random* addition of two hydrated chloride anions. Finally, the addition of water molecules is performed as explained for Configuration A1.

b. Dicationic Cu(II)-G0 Complexes. Configuration B1: Starting with the setup outlined for configuration A1 before the addition of the water molecules, one additional hexahydrated Cu(II) is added *randomly* and the addition is followed by 1 ns of MD. Then two more hydrated Cl^- are added *randomly* to charge balance the system and one additional nanosecond of MD is run. Addition of water is done as described for Configuration A1.

Configuration B2: The initial configuration for these simulations consisted of two Cu(II) ions each one *coordinated to one tertiary amine N (atom type NC) atom in the EDA core, two amide O atoms , and three water molecules* with the G0-OH central dihedral NCCN at about 180° as in its all-trans conformer *tttt*3.[26] MM optimization, as described above, is performed until convergence and followed by MD during an additional nanosecond. After completion, four hydrated Cl^- anions are added *randomly* and MD simulations are run for another nanosecond. Water is added to the system and MD simulations are carried out as explained in the previous cases.

To gain insights about the role of tertiary amines in branching points, DFT optimizations are performed by placing a Cu(II) ion *near to two amide O atoms and the branching N*; the initial configuration resembled that discussed in our previous work.[31] One water molecule completes the equatorial tetracoordination and two others are placed in the axial positions. Two alternative configurations met these initial arrangements differing only in the relative proximity of the hydroxyl terminal groups to Cu(II) and they are referred to herein as *open* and *close* configurations. Finally one more configuration is generated and DFT optimized, where Cu(II) coordinates to one amide O, one hydroxyl O, and four water O atoms (two in equatorial and two in axial positions)—reminiscent of one of the configurations found in our present MD simulations. We attempted optimization of another configuration where Cu(II) coordinates to one amide O atom, three water O atoms in the equatorial plane (O_{eq}), and two water O atoms in the axial sites (O_{ax}), in the presence of another water located in the second shell of the ion but still inside the dendrimer fragment. Optimization of this configuration resulted in a local minimum with one negative value in the Hessian matrix; however, since the magnitude of the corresponding frequency was so small (5 cm^{-1}) its presence should not be a sign of instability, and the results are included in this report.

2.2. Protocol for MD Simulations. As indicated in the previous section, the total simulation time frame depends on each specific configuration, ranging from one to a few nanoseconds. Full-solvent simulations consisted of 400 ps of equilibration followed for collection of trajectories every 200 steps during the last 200 ps of production time. We emphasize that the simulation length of 600 ps used in our full-solvent simulations is justified both by rough estimates of relaxation times of PAMAM dendrimers smaller than fifth generation that are expected to be less than 100 ps—estimate inferred from Monte Carlo simulations[32,33]—and also by convergence achieved in the time evolution of the total energy in our simulations.

We use cubic periodic boundary conditions and account for the long-range electrostatic interactions with the Ewald summation.[34] Although relatively small cutoffs on the order of 12 Å[35] are commonly used, we chose a larger cutoff of 22 Å to achieve a better description of electrostatic interactions.[36] Our longer cutoff is set according to the conventional multiple time-step algorithm[37] in which explicit calculation of forces is implemented in an inner shell of a given radius (of 16 Å) and forces are updated for the outer shell (of 22 Å) every three MD time steps.

The Nose−Hoover[38] thermostat—with 1.0 ps relaxation time—is used to keep the system temperature around 300 K under the NVT ensemble formalism. These computational techniques are used as implemented in the DL_POLY_2 molecular dynamics package.[39]

2.3. LJ Length and Energy Parameters for Cu−Water Interactions. Among the best methods available to investigate chemical details in systems of similar complexity the ab initio MD techniques (such as Car−Parrinello MD[40]) are usually mentioned because they do not require effective potential functions. However, their practical application is limited due to the small size (number of atoms) and time (normally in the order of tens of picoseconds) that can be handled. Modeling Cu(II) hydration[41] with these tools has been questioned[42,43] because of the particular choice of DFT functional and because of the small system size. An alternative method, although also very demanding,[42] is QM/MM MD, which is a molecular dynamics technique that treats a small region of the system with QM and the surroundings with MM by using appropriate force fields.[42] Finally, classical MD methods are still the most popular due to their low computational cost, although they require a careful force field selection and parametrization.

For Cu(II) hydration, we recognize that within the context of classical MD simulations we cannot capture quantum-mechanical effects such as the Jahn−Teller distortion, which is known to take place in the process of Cu(II) complexation to water. However, since our interest is to get a reasonable picture at a modest computational cost, we chose a simple set of force fields, namely a two-body Coulombic plus Lennard-Jones potential, to describe the Cu(II)−water interactions, and placed special efforts in the force fields parametrization.

Thus, the ion is modeled with a point charge of 2^+—a reasonable assumption in light of recent research that has detected no other species but Cu(II) when forming complexes to dendrimers[19]—with length and energy parameters given by the LJ potential to account for weak van der Waals interactions. To determine the LJ parameters for the Cu−water interaction, the nonbonded distance and energy parameters corresponding to Cu^{1+} in tetrahedral coordination as reported in the UFF[29] potential were taken as initial values for our length and energy LJ parameters, respectively. Then, maintaining the energy parameter unchanged, the length parameter was modified until obtaining a 6-fold coordination (1st shell running coordination number of six) and the first peak position in the Cu−OW radial distribution (Figure 1) matching both reported average values of 2.12 Å[44,45] and our own DFT calculations where the average ($4\ O_{eq} + 2\ O_{ax}$)/6 amounts to 2.12 Å—although our DFT calculated geometry (B3LYP/6-31g(d) with LANL2DZ[30] with pseudopotentials only for Cu) is not strictly a distorted octahedron: the equatorial plane forms an angle different than 90° with the axial axis. The optimization of the LJ length parameter was done with MD simulations for a system of one ion and 523 water molecules, with cutoff of 8.5 Å, and the initial configuration was given by a box-centered cation.

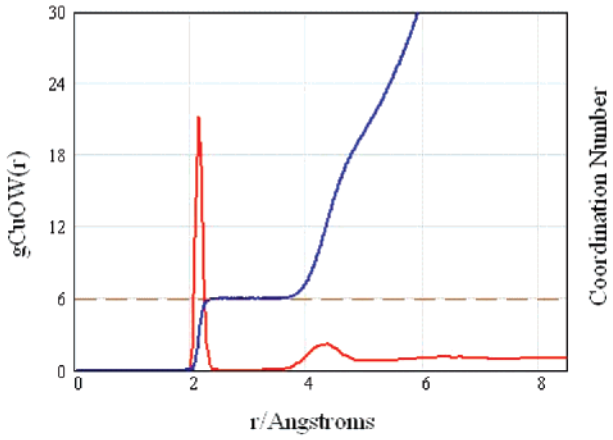

Figure 1. Radial distribution function (red line) and running coordination number (blue line) obtained from classical MD simulations for the Cu(II)−water (Cu(II)−OW) interactions as modeled in this work.

The parametrization of the two-body potential function to describe the Cu(II)−water interactions has been discussed by several authors. Rode and Schwenk[42] evaluated two approaches: classical pair + 3-body potential correction and a QM/MM approach. Our results are in agreement with theirs in the position of the $g_{Cu-OW}(r)$ first peak maximum (2.12 Å) and first shell coordination number of 6.0. However, we obtain a higher peak height, about 20, compared with their values of 15 and 10 for the classical pair potential + three-body correction and for the QM/MM approach, respectively. Two main differences may account for such discrepancy: the water model used by these authors is the BJH-CF_2[46] whose geometry corresponds to gas-phase water, whereas the SPC/E used in our work is a model for liquid water that has a longer O−H bond length and angle, representing the molecular properties of water in the liquid state. The second difference is their use of a three-body correction to the two-body potential. In their simulations and ours, the hydrated complex obtained with the classical potentials corresponds to a hexahydrate in octahedral configuration. But in their QM/MM model, these authors obtain an alternative octahedral distorted (4+2) configuration, showing equatorial and axial water molecules around the Cu(II) ion. Experimental residence times of water in the first shell of the ion have been reported to be 230 ps at 298 K as determined by NMR techniques,[47] although it was argued that the technique might not to be accurate in the picosecond time scale.[42] It is speculated that due to the very short lifetime of a Jahn−Teller distortion the experiments cannot distinguish between alternative configurations, so the measurement corresponds to an average of all geometries. As our potential does not reproduce Jahn−Teller effects we do not attempt to calculate any residence time of water in the Cu(II) first coordination sphere.

Finally, as the O−O LJ parameters are known for the SPC/E water model, the Lorentz−Berthelot rules were applied yielding a Cu−Cu length parameter of 2.9283 Å. The Cu−Cu energy parameter taken from UFF[29] is 0.050 kcal/mol.

3. Results and Discussion

In this section we analyze radial distribution functions (rdfs) and the time evolution of distances between the ion and the various sites, obtained from MD simulations for the complete systems, as well as DFT calculated bond distances and energies for a 38-atom dendrimer fragment in contact with the hydrated ion.

From experimental work done in Cu(II)−dendrimer complexes it is not clear whether Cu(II) coordinates to six or five atoms. Some studies state[19,48] that either trigonal bipyramidal or base pyramidal geometries are more likely to be found in such complexes. On the other hand, Diallo et al.[14] propose two-site models that implicitly assume hexacoordination and other experimental work suggests a (4+2) coordination for Cu(II) when present in dilute aqueous solutions of similar complexes.[49,50] This debate is reminiscent of the one held for Cu(II) in aqueous solutions where supportive evidence for penta-[41] and hexacoordination[42] has been presented. In line with the currently accepted 6-fold coordination for Cu(II) in water[43,51] we assume that Cu(II) will retain its hexacoordination when forming complexes with molecules such as peptides[49] and dendrimers.[14] Table 1 displays the identity of the nearest six atoms to Cu(II) as well as their time averaged distances to Cu(II) obtained from the MD simulations initiated as described in section 2.1.

Closeness to both the amide oxygen (atom type O) and hydroxyl oxygen (atom type OT) is evident in all cases except in configuration A2 (two amide O atoms are the closest atoms), and in one of the two Cu(II) atoms in configuration B1. Moreover, when coordination to O and OT exists, the Cu(II)−hydroxyl O distance is slightly shorter than the distance to the closest amide O atom except in B2, and in the DFT optimized geometry of a 38-atom fragment Cu(II)−$(H_2O)_4$ (Figure 5d), where the opposite trend is observed. This discrepancy is discussed in section 3.3. The presence of two to five water molecules in the first coordination shell is evident. It is also noticeable in all the cases that even the farthest Cu(II)−non-OW distance, which ranges 1.94 to 1.97 Å, is closer than the closest Cu(II)−OW distance, which ranges 2.15 to 2.17 Å. However, in configuration A2 the closest Cu(II)−NC distances average 2.78 and 2.52 Å (their average is shown in Table 1) and are longer than any of the Cu(II)−OW distances in the first shell. Further, the time evolution (Figure 2) of the Cu(II)−dendrimer atom distances in this system suggests a loose coordination to these two tertiary amine N sites which contrasts with the steady behavior of the bond distances Cu(II)−OW, Cu(II)−OT, and Cu(II)−O observed in the rest of the configurations such as A1 shown as an example (Figure 3). Thus, these results indicate that proximity to the amide O and hydroxyl O atoms are preferred by the Cu(II) ion.

3.1. Cu(II) Coordination to Tertiary Amines in Core Site and Branching Points. Cu(II)−NC rdfs can reveal information on the coordination of Cu(II) to the core site. From the rdfs (not shown) it is found that only in one of the configurations (A2) do the Cu(II) ions remain 2.43 Å close to the tertiary amine in the EDA core (atom type NC). This value is different from that reported in Table 1 (2.65 Å), which corresponded to the average of the closest average distance found for each of the NC atoms. Instead, the rdf value is the statistically averaged density of NC atoms (relative to the bulk density of NC atoms) found at 2.43 ± 0.05 Å. The second closest Cu(II)−core distance found in one of the dicationic complexes, namely configuration B2, corresponds to two small peaks of approximately the same height at 3.98 and 4.18 Å. In the rest of the configurations the Cu(II)−NC highest peak is found between 5.58 and 5.93 Å and between 6.43 to 7.23 Å suggesting that the NC atoms are much less involved in binding to Cu(II), as expected for low generation dendrimers.[52]

Although G0 dendrimers have no branching points, DFT calculations in dendrimer fragments can provide insights on how tertiary amine in branching points binds to Cu(II) especially when water is coordinated to the ion. Our DFT calculated bond distances Cu(II)−N3 of 2.03 (for the naked ion) and 2.05 Å

TABLE 1: Time Averaged Bond Distances (Å) of the Cu(II) and the Six Closest Atoms[a]

	configuration						
n-closest atom	A1 Cu(II)	A2 Cu(II)	A3 Cu(II)	B1		B2	
				Cu(II)[a]	Cu(II)[b]	Cu(II)[a]	Cu(II)[b]
1st	1.95 (OT)	1.92 (O)	1.92 (OT)	1.94 (OT)	1.95 (O)	1.91 (O)	1.93 (OT)
2nd	1.97 (O)	1.92 (O)	1.94 (O)	1.97 (O)	2.15 (OW)	1.95 (OT)	1.93 (O)
3rd	2.15 (OW)	1.94 (O)	2.17 (OW)	2.15 (OW)	2.15 (OW)	1.95 (O)	1.95 (O)
4th	2.16 (OW)	2.16 (OW)	2.17 (OW)	2.15 (OW)	2.15 (OW)	2.17 (OW)	2.16 (OW)
5th	2.16 (OW)	2.18 (OW)	2.17 (OW)	2.15 (OW)	2.16 (OW)	2.18 (OW)	2.17 (OW)
6th	2.17 (OW)	2.65[b](NC)	2.17 (OW)	2.17 (OW)	2.16 (OW)	2.18 (OW)	2.18 (OW)

[a] OT, hydroxyl O; O, amide O; OW, water O; NC, tertiary N in the EDA-core. Superscripts "a" and "b" designate two different Cu(II) ions in the dicationic complexes. [b] Average of the two closest average Cu(II)−NC bond distances (Figure 2).

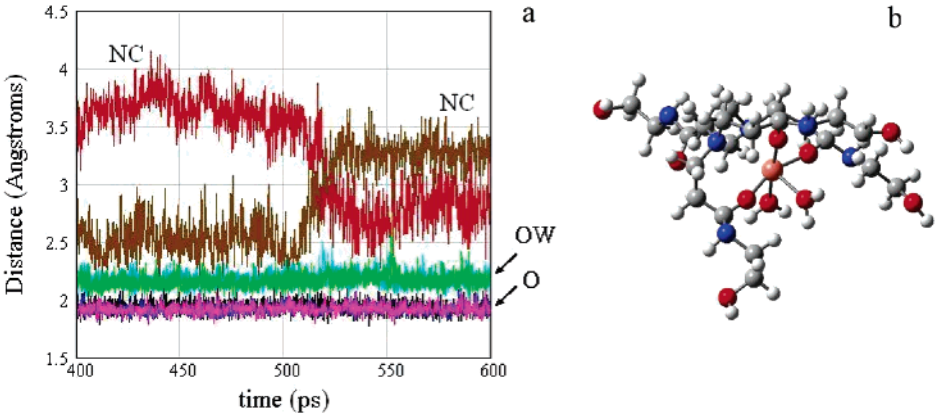

Figure 2. (a) Time evolution for Cu(II) coordinated to three amide O (O), two water O (OW), and one core tertiary amine N (NC) atom—configuration A2. (b) Snapshot after 600 ps of MD. The plot suggests that coordination to core N switches identity approximately every 100 ps.

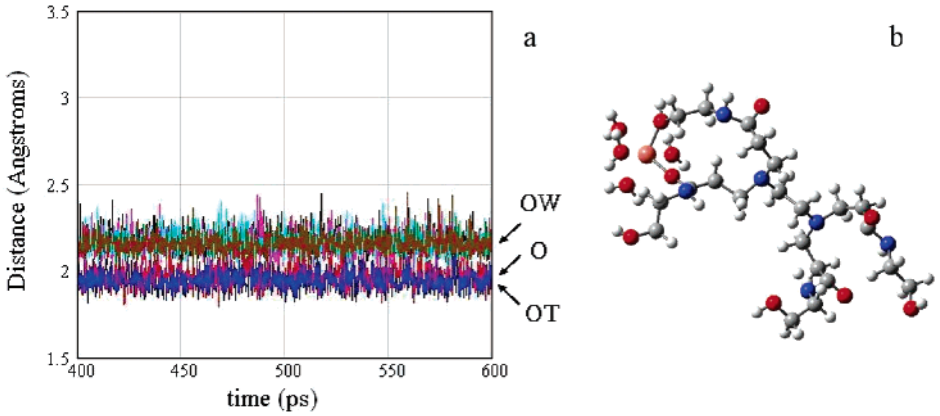

Figure 3. (a) Time evolution of the distances between Cu(II) and one amide O (O, red line), one hydroxyl O (OT, blue line), and four water O (OW) atoms —configuration A1. (b) Final configuration after 600 ps of MD.

(for the ion hydrated with three water molecules) seem to agree more closely with experimental results for Cu−N distances in the range 2.01−2.02 Å in like complexes[50] than with the single Cu(II)−NC bond distance (>2.45 Å) obtained by MD for configuration A2. The calculated charge distribution (Mulliken charges) in G0 reported in our previous work[26] yields a value of −0.39 for N of the NC site—tertiary amine in EDA core—whereas in this present work it was −0.38. For a G1 branch, similar calculations yield −0.40 for N3—tertiary amine in a branching point.[53] Therefore as there are no significant differences between the calculated charges for N3 and NC based on the optimization of a dendrimer or a dendrimer fragment we suggest that tertiary amines in EDA core and tertiary amines in branching points ought to be chemically identical, although the nature of the environment surrounding the particular site is different in each case. In contrast, the present DFT calculations which are based on a 38-atom dendrimer fragment in contact with Cu(II)−$(H_2O)_3$ yield a higher charge for the branching N in the DFT fragment than those obtained for the dendrimers: for the open and close configurations they are −0.61 and −0.63, respectively, which also differ from the DFT value (−0.52) calculated for the 38-atom fragment Cu(II)−$(H_2O)_4$. This may suggest that the hydrated ion induces polarization in the tertiary amine, an effect that is not taken into account in our force field, although these two sets of DFT charges may be lower if we had modeled a complete dendrimer, since in our calculations the missing half of the dendrimer was substituted by an H atom making the N site resemble more a secondary than a tertiary amine. Thus, the agreement of the Cu−N distances with experimental data suggests that the DFT model may be a fair representation of the Cu−N3 interaction in higher generation dendrimers outer pockets, whereas our MD model reasonably describes the solvent and dendrimer effects found in G0 where such tertiary amines in branching points do not exist.

In addition, it is known that the environment for the tertiary amines in the EDA core is hydrophobic; therefore, in conditions where the dihedral angle NCCN opens up to about 180° [31] these two NC atoms would become far from one another and consequently the cooperative effect between them that enhances coordination to the ion weakens. This is in contrast with gas-phase calculations[31] that predicted a stable configuration for the ion at this location, where the dendrimer was represented by a fragment that intended to emulate the core region but had a lower value—about 64°—for the dihedral angle NCCN. Instead, the full solvent MD results yield a value of 180° for the NCCN dihedral angle, which may be the result of a fair representation of the solvent effect in G0 dendrimers.

Experimental evidence of Cu(II) binding to N atoms has been suggested by several authors. For instance, release of Cu(II) to bulk solution upon protonation is often interpreted as proof that binding of Cu(II) to tertiary amine may have occurred prior to protonation.[14] Unfortunately, the majority of these studies have been done on amine-terminated dendrimers, and since terminal primary amines (N1) have proven better ligands than tertiary amines (N3) it cannot be concluded that Cu(II) was exclusively coordinated to tertiary amine sites. However, it cannot be inferred that prior to protonation Cu(II) was bound *solely* to N1, because these functional groups may preferentially bind protons rather than Cu(II). Instead, we propose that protonation can disrupt not only interactions of Cu(II) with both amine sites (N3 and N1), but also any possible type of Cu(II)−dendrimer atom interaction because of the electrostatic repulsion between Cu(II) and protons that can be adsorbed in the interior and exterior of the dendrimer. Thus, as suggested by an EPR study, the picture is more complex involving binding to the $-NH_2$ surface groups and tertiary amines,[16] although such an assumption has also been challenged by a recent study that proposed involvement of other atom sites such as amide N.[17] This involvement was suggested on the basis that it is less likely to have Cu(II) simultaneously coordinated to N3 and N1 given the relative long distance between N1 and N3. In addition, our DFT calculations (see discussion in the Full Solvent Effect section) suggest that Cu(II) is able to bind simultaneously to tertiary amines and to the amide O atom thus implying the existence of a cooperative effect of other atom sites in binding, at least for PAMAM−G0-OH dendrimers.

3.2. Cu(II) Coordination to Amide Group. Coordination to either O or N amide atoms has not been inferred from experimental work,[14] although some evidence has been suggested by interpretation of FT EXAFS measurements[17] as mentioned in the previous section. However, assignment of coordination to either O or N is difficult[14] because of the acknowledged uncertainties inherent to the FT EXAFS fitting technique such as similarity in backscattering functions for O and N atoms which are close in atomic weight, size, and electronic configuration.[19] Also, the reported measurement accuracy of ±0.02 Å [14] may not reflect the errors incurred in the FT EXAFS fitting relying on the assumption of bond length invariance within the dendrimer structure[17] (i.e., C−C, C−N, C═O, and other bond lengths retain their typical values found in smaller molecules[54] thus neglecting the effect of environmental variables such as the presence of Cu(II), solvent, and branch folding, among others that may affect those bond lengths). For instance, our DFT study shows a lengthening of the C═O bond when Cu(II) binds to the amide O atom in the presence of water. The calculated C═O bond lengths in a 38-atom fragment interacting with Cu(II) and also with Cu(II)-$(H_2O)_3$ are 1.28 Å for the naked ion and 1.27 Å for the solvated ion, a difference of 0.05 Å from the accepted C═O bond length of 1.23 Å.[54] Thus, we suggest that DFT calculations could help in future refinements of EXAFS studies as reported recently.[55] Another factor that may affect the EXAFS results is the state of the sample used in the analysis, since changes in the bond distance Cu(II)−water O when switching EXAFS measurements in fluorescence mode from powder to slurry[56] have been reported. In the following sections we discuss our results for Cu−amide interactions and relate them to experimental results.

a. Cu−Amide N Distance. Assuming that the likelihood of finding the Cu(II) ion near the position of the highest rdf peak is the maximum, we observe that the position of this highest value for Cu(II)−N2 (Cu(II)−amide N) rdfs ranges from 3.08 to 3.98 Å for the single Cu(II) ion coordination configurations. For the cases where two Cu ions are present 3.93 and 5.23 Å are found for configuration B1, whereas two peaks of nearly equal height are found at 3.48 and 3.98 Å in configuration B2. The time evolution of the Cu(II)−N2 bond distances for configuration A2 shows a steady behavior with values that range from 3.83 to 3.91 Å confirming that Cu(II) is not as close to the amide N as it is to other atom sites. Also our DFT bond distances (Table 3) reveal that this proximity is at least in the range 3.55 to 4.05 Å, which is almost twice the distance to coordinating atoms. Binding to the amide N when Cu(II) or other ions bind to dendrimers was suggested in our previous study[31] but those results cannot be extrapolated to this case because a different surface group was used and the solvent effect was not accounted for. Therefore we cannot attribute a participation of the amide N in Cu(II) coordination as suggested by the EXAFS work.[17]

b. Cu−Amide O Distance. The first and highest peak for the Cu(II)−O (Cu(II)−amide O) rdfs is located at 1.93 Å with the only exception being configuration A1 where it is found at 1.98 Å. The sharpness and height of these peaks suggest that these atoms remain close to Cu(II) during the simulation course. The time evolution of bond distances provides an average value that is slightly more accurate than the information given by the calculated rdfs, which have a precision of ±0.05 Å. Thus, the time evolution of the Cu(II)−amide O distances indicates that they range from 1.91 to 1.97 Å, in fair agreement with the rdf values. The difference in the value of the shortest distance (1.91 vs 1.93 Å) reveals the presence of individual amide atoms located at distances closer than the position of the rdf first peak.

Our DFT calculations show that for the 38-atom fragment the Cu(II)−O bond distance is 1.85 Å in the absence of water, but upon addition of three water molecules this equatorial bond distance enlarges up to 1.98−1.99 Å (vide infra)—in the rest of configurations we found a Cu−O bond distance of 1.99 Å also—in closer agreement with experimental results for the Cu−N distances (which may be Cu−O distances considering the EXAFS interpretation problem discussed above) reported in works by Tran et al.[17] and Diallo et al.[14]

Tran et al. also reported ^{13}C NMR and ^{1}H NMR results and attributed broadening of the C═O signal to coordination of the nearby Cu(II) ion to the amide N; however, the same phenomenon could also be attributed to Cu(II) coordination to the amide O. Thus, interpretation of experimental data is not conclusive. Tran et al.[17] disregarded coordination to amide O stating that four or five N atoms are located at 1.98 Å and one N or O at 2.84 Å in the first Cu(II) coordination sphere.

Comparison of FT EXAFS fitted Cu(II)-equatorial atoms with literature values of Cu(II)−O bond distances for like complexes is commonly used to rule out coordination to amide O. Diallo et al.[14] followed this criteria and although they acknowledge

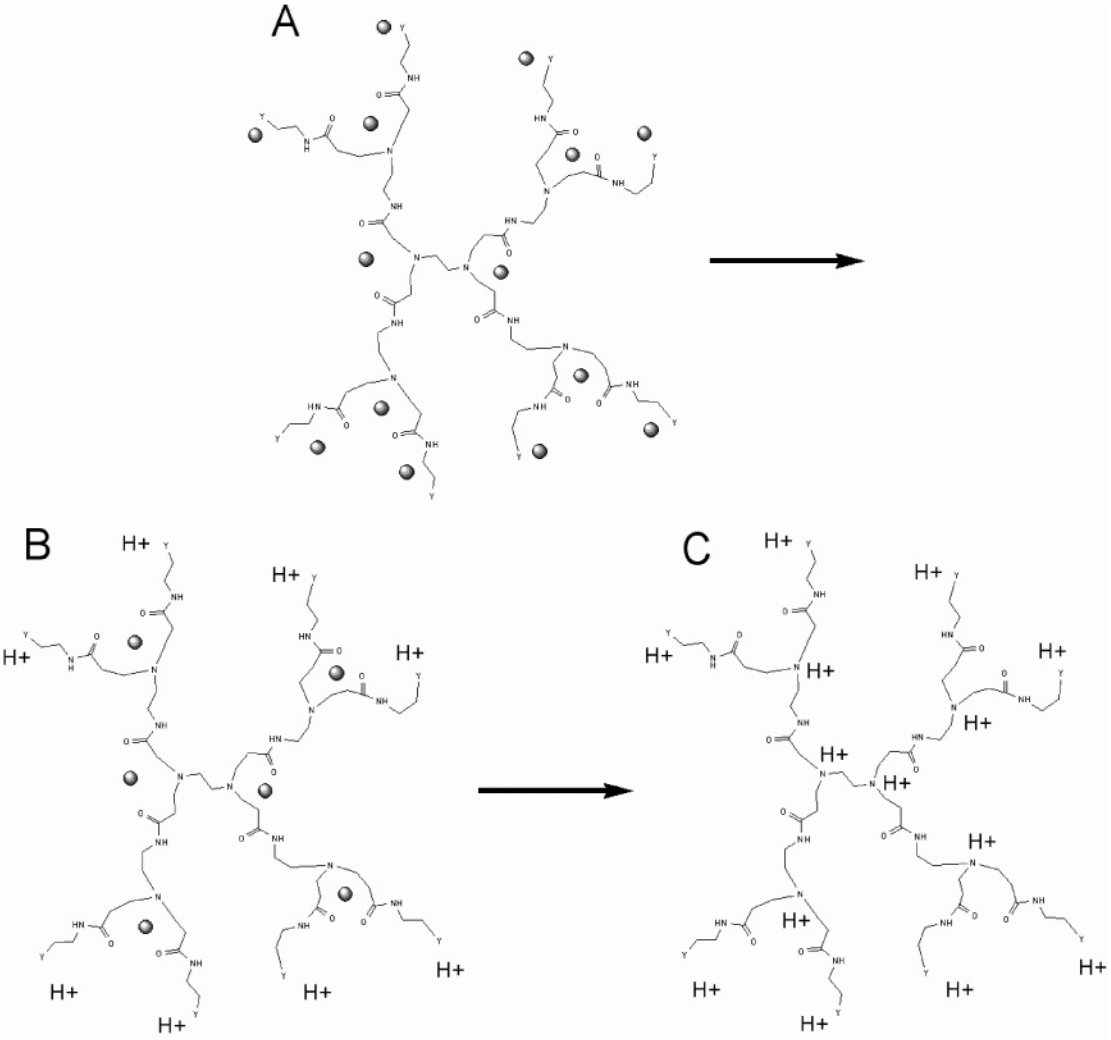

Figure 4. Scheme of the expected protonation effect on Cu(II) complexation. (A) A high pH scenario: no protons are present either inside or outside the dendrimer, therefore Cu(II) can reach all the available coordination sites either individually—as it may be in the terminal groups, specially primary amines—or cooperatively. (B) A slightly departed from neutral pH scenario: here either the terminal groups have become protonated—as in primary amines—or the protons remain very close to them preventing Cu(II) from reaching those sites due to electrostatic repulsion. (C) A low pH scenario: tertiary amines are protonated, thus individual site coordination—as suggested for tertiary amines—and cooperativity between atomic binding sites—like amide O atom with tertiary amine—are disrupted due to protonation. Even if the tertiary amines were not cooperatively involved with amide O atoms, we speculate that the possible presence of protons in the void water pools may disrupt coordination to pure amide O sites in addition to disrupting complexations of Cu(II) to other dendrimer sites. Note: Even though a G1 dendrimer is depicted in our scheme, neither this particular generation nor the number of Cu(II) particles pretend to represent a quantitative assessment of particle load. Y: functional or surface group.

that validation of their models is a pending issue they compared their EXAFS FT fittings (with assumed Cu−N distances of 2.00 ± 0.02 Å) to Cu(II)−O bond distances of 1.93−1.96 Å referring to published literature,[49,50,56] although the data described in those articles hardly ever support their assertions. In another set of experiments, Diallo et al.[14] conducted a pH-regulated Cu(II) uptake experiment in amido-terminated dendrimers and as no uptake of Cu(II) was observed at pH 5.0 they concluded that amido groups are unable to bind Cu(II). However, it is known that amido groups, which bear negative partial charge in the amide oxygen, can attract free protons to their neighborhood forming strong hydrogen bond interactions.[57] Therefore if protons are found sorbed in the dendrimer exterior, electrostatic repulsion between them and the potentially approaching Cu(II) ions can provide an alternative interpretation to the inability to find Cu(II) sorbed to the dendrimer, instead of being a signal of the absence of Cu−amido group interactions.

We conclude that the exposed arguments inferred from experimental information regarding lack of coordination to the amide O site are not convincing; instead fair agreement between experimental Cu−equatorial bond distances and our MD calculated Cu−O bond distances suggests coordination to amide O.

3.3. Cu(II) Coordination to End Group Hydroxyl O. The first and highest peak location for all the configurations except for A2 is found at 1.93 Å. Table 1 shows that the shortest bond distance obtained by averaging its time evolution for individual atoms ranges from 1.92 to 1.95 Å whereas the DFT bond distance found for the 38-atom fragment coordinated to four water O, 1 amide O, and 1 hydroxyl O is 2.04 Å. Therefore there is a discrepancy between our DFT and MD values amounting to 0.09 Å. One reason for such a discrepancy might be attributed to inaccuracies in the LJ parameters used for hydroxyl O, taken from the Dreiding force field, which may not faithfully describe a hydroxyl O. However, we also acknowledge that the MD and DFT models are not totally comparable (Figure 5, parts a and b and parts c and d).

3.4. Cu(II) Coordination to Water. A close look at the Cu−water oxygen (Cu(II)−OW) rdfs (not shown) in our complete

system yields very well resolved peaks similar—in resolution and shape but not in height—to those observed in the hexahydrate Cu(II)−OW rdfs (Figure 1). Thus, for the first and highest peak we obtain 2.125 (configurations A1 and B1) and 2.18 Å (configurations A2, A3, and B2). Average values of Cu(II)−OW distances were also reported in Table 1, and their time evolution in Figures 2 and 3 with values that range from 2.15 to 2.18 Å.

From our DFT calculations we observe that the Cu(II)−water O bond distances differ depending on where water coordinates and on the configuration details. For instance, the equatorial water in the 38-atom fragment Cu(II)−$(H_2O)_3$ complex sits 2.06 Å away from Cu(II) in both the open and closed configuration whereas in the 38-atom fragment Cu(II)−$(H_2O)_4$ the two water molecules locate at 2.00 and 2.03 Å and at 2.01 Å, as an average, in the 38-atom fragment Cu(II)−$(H_2O)_6$. On the other hand, the axial waters in the 38-atom fragment Cu(II)−$(H_2O)_3$ are, on average, found at 2.39 and 2.42 Å for the closed and open configurations, respectively, and 2.46 Å for the 38-atom fragment Cu(II)−$(H_2O)_6$, whereas two axial waters in the 38-atom fragment Cu(II)−$(H_2O)_4$ complex are found at 2.21 and 3.38 Å. The latter value differs significantly from what seems to be a typical bond distance for axial waters.

Coordination to axial sites with either one[17] or two[14,19] ligands have been proposed based on FT EXAFS spectra of Cu(II)−dendrimer solutions. Although the identity of those ligands has not been unambiguously determined,[19] Diallo et al. suggest those ligands are water based on their estimated Cu−O bond distances of 2.32 and 2.39 Å found for PAMAM G1 and G5.[14] D'Angelo et al. reported two axial Cu−O distances of 2.40 ± 0.06 Å in bi(glycinato)−Cu(II) complexes.[49] These distances are larger by 0.11 Å than those observed in EXAFS of Cu(II) aqueous solutions.[45,51] Evidence for equatorial coordinated water was found in the monoglycinato copper complex. [49]

Since our DFT calculations cannot reproduce the octahedral distorted structures, we cannot report a unique Cu−O bond distance. Instead our results indicate that the Cu−O equatorial distance ranges from 2.00 to 2.06 Å and the axial distance ranges from 2.21 to 2.40 Å. Clearly the complexity introduced by the Jahn−Teller effect makes difficult not only accurate experimental determinations but also calculations of complexes with DFT as we attempted in this work.

From the analysis of the MD trajectories a predominance of water oxygen (atom type OW) is found in the first coordination shell. This should not be surprising as it is known that the G0 dendrimers are regarded as open dendrimers[58] so water can easily reach the dendrimer sites as mentioned by Ottaviani et al.[52] In summary, coordination of Cu(II) with O atoms is interesting because it is reminiscent of a tendency for Cu(II) to recover coordination to O atoms as in a hexahydrated Cu(II) complex. However, we do not discard coordination to N atoms, instead we suggest that the type of atom sites involved in binding of Cu(II) would depend on the solvent used and dendrimer size, surface group, and shape, among other factors.

3.5. Full Solvent Effect. In this section we provide details about DFT optimized configurations of the 38-atom fragment complexed with hydrated Cu(II) and make some comparisons with configurations found in the MD simulations. Table 2 displays the energetic characteristics of Cu(II) in various degrees of hydration complexed to a 38-atom dendrimer fragment, with the main distances of Cu(II) to its closest atoms indicated in Table 3, some of which have already been discussed in the preceding sections. A comparison between a fully solvated system (Figure 5a, MD results) and one where only three water molecules are present (Figure 5b, DFT results) indicates that despite the presence of bulk water in the surrounding environment, "closed" configurations, where the dendrimer branches contribute to a "cage" effect, can continue being energetically favorable as compared to "open" structures. In fact, a difference of ∼6 kcal/mol is found by our gas-phase DFT calculations in favor of the closed over the open structure (Table 2). The strong binding of Cu(II) to the dendrimer fragment takes place by attachment to two amide O atoms and the branching N atom (Figure 6a and Table 3), and such a structure is maintained when Cu(II) is hydrated by three water molecules as in the open and closed configurations (Table 3). However, when Cu(II) is hydrated by four or six water molecules (Figures 5d and 6b), the coordinations to N and to one of the amide O atoms are lost and substituted by coordination to water oxygen atoms.

TABLE 2: DFT Energies Calculated at B3LYP/6-31g(d)[a]

molecule or fragment	energy (au)	no. of H_2O	ZPE (au)	$E_{binding}$ (kcal/mol)
D38AF	−858.84591	N.A.	0.32954	N.A.
H_2O	−76.40895	N.A.	0.02117	N.A.
Cu(II)	−195.0649	N.A.	0.00000	N.A.
D38AF Cu(II)	−1054.52262	0	0.33600	−379.97
D38AF Cu(II)−$(H_2O)_6$	−1513.14444	6	0.48840	−469.84
D38AF Cu(II)−$(H_2O)_4$	−1360.26345	4	0.43587	−436.52
D38AF Cu(II)−$(H_2O)_3$				
closed	−1283.86908	3	0.41325	−446.57
open	−1283.85458	3	0.40835	−440.49

[a] $E_{binding}$ = {(energy + ZPE of complex branch/ion) − [energy ion + (energy + ZPE of reference fragment)]} in kcal/mol. ZPE correction scaling factor: 0.9806.[59] D38AF: 38-atom-dendrimer fragment.

In contrast to Figure 5a, the single-ion attachment shown by Figure 5c illustrates a more open configuration where the ion attaches to the terminal OH group and to one amide O atom, retaining four of the six water molecules present in the bulk water hexahydrate.

It is interesting to observe that the sixth water in Figure 6b inserts in the void formed by the two dendrimer branches, and coordinates with hydrogen bonds to the amide O and hydroxyl O atoms. One may speculate that this water molecule may have been separated from a Cu(II) hexahydrate that lost one of its water molecules in the first shell to bind to one amide oxygen. Thus, we analyze what could be the reasons for such exchange. First, our DFT calculations allow us to estimate that upon complexation of a Cu(II) hexahydrate to the 38-atom fragment—resembling an outer dendrimer pocket—the release of one of its water molecules to bind an amide oxygen in the fragment stabilizes the complex. Also from our DFT Cu(II) hexahydrate calculations we observe that the Cu−O equatorial and axial distances average 2.04 and 2.29 Å, respectively, and from Table 3 we observe that in the Cu(II)-fragment complex the Cu−O equatorial are even shorter, although the Cu−O axial are larger than in the Cu(II) hexahydrate. Therefore a combined effect of shorter and stronger bonds, H-bonding enhanced stability, and chelate effect can explain why Cu(II) hexahydrates will more likely lose some of their coordination waters to bind to the dendrimer.

The MD snapshots shown in Figure 5c and also those in Figures 3b, 2b, and 5a correspond to stable configurations obtained after 600 ps of full-solvent simulations—they are representative of their respective equilibrated systems initiated from configurations A1, A2, and A3 (vide supra). Figure 7a and 7b illustrate configurations of the two-ion attachment to G0-OH; in both cases a strong participation of the dendrimer branches is observed.

TABLE 3: Bond Distances of Cu(II) and the Closest Atoms from DFT Calculations[a]

complex	N3	O[a]	O[b]	OT	OW[a]	OW[b]	OW[c]	OW[d]	OW[e]	N2
D38AF Cu(II)	2.03	1.85	1.85							
D38AF Cu(II)−$(H_2O)_6$	5.26	1.99			2.05	1.98	2.00	2.32	2.60	4.05
D38AF Cu(II)−$(H_2O)_4$	5.86	1.99		2.03	2.00	2.03	2.21	3.38		3.55
D38AF Cu(II)−$(H_2O)_3$										
closed	2.05	1.99	1.99		2.06	2.28	2.49			4.01
open	2.05	1.98	1.98		2.06	2.40	2.44			

[a] Superscripts a−e are used to designate different atoms of the same type (two different O and five different OW). N3, tertiary amine; O, amide oxygen; OW, water oxygen; N2, amide nitrogen.

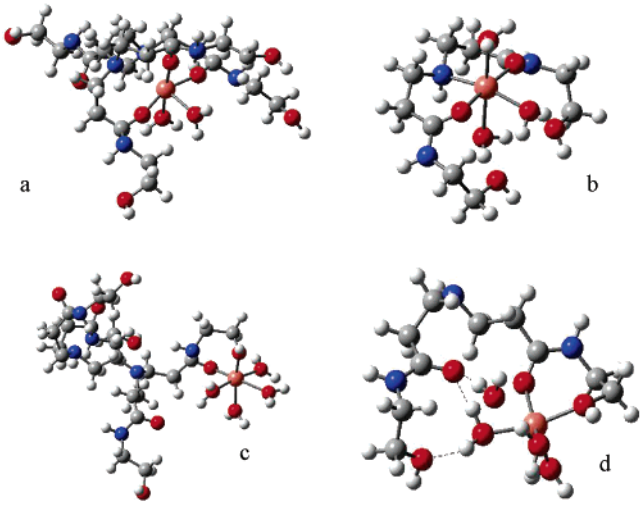

Figure 5. (a) Full-solvent MD final configuration A2: Cu(II) is coordinated with two amide O atoms, one tertiary N in the EDA core, and one water O atom in the equatorial position. Branch folding places one amide O atom in the axial position (the other is occupied by one water O). For clarity, water molecules other than those in the first coordination sphere of the ion are not shown. (b) 38-atom fragment Cu(II)−$(H_2O)_3$ closed DFT (optimized structure): Cu(II) coordinates in a fashion similar to configuration A2 except that the branch folding effect is obviously not reproduced; another water O substitutes the amide O of the dendrimer branch. Here the equatorial water and one of the axial waters form hydrogen bonds R′−CH_2−(OH)- - -HOH- - -(OH)−CH_2−R′ to both hydroxyl O atoms with lengths of 2.12 and 1.99 Å, respectively. These H-bonds may explain its enhanced stability compared to that of the "open" configuration. (c) Full-solvent MD final configuration A3: Cu(II) is coordinated to one amide O, one hydroxyl O, and four water O atoms. (d) 38-atom fragment Cu(II)−$(H_2O)_4$ (optimized structure): coordination to one amide O, one hydroxyl O, and two water O atoms in the equatorial plane and one water in the axial position. One of the equatorial waters forms an H-bond (dashed lines) as R′−CO- - -HOH- - -(OH)−CH_2−R at 1.81 (with carbonyl O) and 1.81 Å (with hydroxyl O). The fifth water is in the quasiaxial position (bond distance larger than the typical Cu−O axial bond distance) and forms H-bonds with one amide O atom at 1.78 Å and with the equatorial water at 1.60 Å.

3.6. Interactions of Cu(II) with Other Cu(II) Ions and Counterions. *a. Cu(II)−Cu(II) Distance.* We are not aware of any other work that has found coordination of two Cu(II) ions to a single G0 dendrimer in the presence of counterions and solvent. The Cu(II)−Cu(II) rdfs show a broad peak centered at about 12.5 Å with a width of about 5 Å (measured at the bottom of the peak) for configuration B1 whereas for configuration B2 a slightly narrower but sharper peak with height twice the aforementioned is observed at 10.88 Å. The time averaged distance Cu(II)−Cu(II) over all the configurations yields 12.6 and 11.3 Å for B1 and B2 configurations, respectively. Thus, the results are not in agreement with the findings of Diallo et al.:[14] Cu(II)−Cu(II) coordination number of 1.9 and separation distances of 3.0 Å for G1-NH_2. The calculated behavior may be partially explained by electrostatic repulsion but also by solvent screening, thus suggesting that the solvent plays an important role in stabilizing up to two Cu(II) ions in low generation dendrimers.

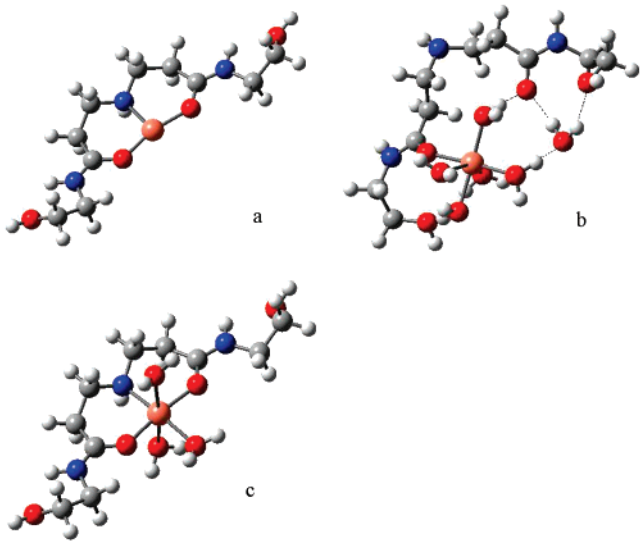

Figure 6. DFT optimized configurations. (a) 38-atom fragment Cu(II): cooperative effect of two amide O atoms to the branching N is evident. (b) 38-atom fragment Cu(II)−$(H_2O)_6$: coordination to one amide O and five water O atoms (3 equatorial and 2 axial). Water interacts with dendrimer atoms forming H-bonds: R−CH_2−(OH)- - -H, length 1.83 Å. The sixth water molecule sits in the second coordination shell and forms two hydrogen bonds (dashed lines) R′−C═O- - -HOH- - -(OH)−CH_2−R in the adjacent branch at 1.81 (amide O) and 1.94 Å (hydroxyl O). (c) 38-atom fragment Cu(II)−$(H_2O)_3$, open configuration: coordination to one branching N, two amide O, and one water O atom in the equatorial plane and two water O atoms in the axial positions.

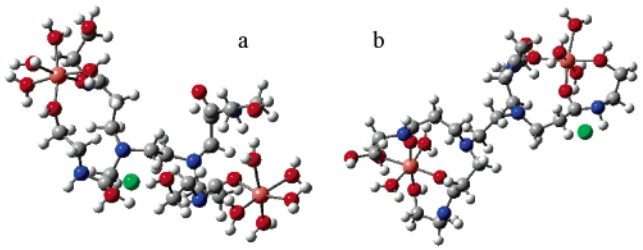

Figure 7. Snapshots obtained after 600 ps of full-solvent MD trajectories. For clarity, water molecules beyond the ionic first coordination shell are not shown. (a) Coordination of one Cu(II) to an amide O, an hydroxyl O, and four water O atoms and another Cu(II) to one amide O and five water O atoms in the opposite part of the dendrimer that remains open. Two branches and their environment can at least hold one Cu(II). (b) Coordination of both Cu(II) to two amide O, one hydroxyl O, and three water O atoms. Again the flat configuration enables the attachment of two branches to each ion. The green atoms are Cl^- counterions.

Nevertheless we should exercise caution with this assertion as this study reveals that a monoionic charged complex could be stable as suggested by results from configuration A2 where

TABLE 4: First Peak Locations (Å) and Respective Peak Heights (dimensionless) for OT−HW, O−HW, N2−HW, and NC−HW Radial Distribution Functions[a]

	OT−HW		O−HW		N2−HW		NC−HW	
configuration	position	height	position	height	position	height	position	height
A1	1.68	1.02	1.73	1.05	1.93	0.27	1.93	0.06
A2	1.68	1.38	1.73	0.37	1.88	0.12	1.83	0.14
A3	1.68	1.08	1.73	1.11	1.93	0.27	1.98	0.007
B1	1.63	1.07	1.73	0.66	1.88	0.24	1.98	0.017
B2	1.68	0.70	3.13	0.53	1.88	0.09	1.93	0.219

[a] OT, hydroxyl O; O, amide O; N2, amide N; NC, tertiary amine in EDA core.

an increased chelate effect (three branches coordinating a single ion) is clearly observed. Consequently a final word on this issue cannot be given yet.

b. Cu(II)−Cl and Cl−Cl Distances. The highest peak locations in the Cu(II)−Cl rdfs for configurations A1, A2, A3, B1, and B2 are 16.93, 9.38, 13.28, 6.68, and 6.53 Å, respectively. It is remarkable that only in one of them (B2) the peak is sharp and nearly 4-fold larger than in the others. The Cu(II)−Cl distances in the single ion configurations (A1 to A3) indicate that the counterion is not significantly attracted by the Cu(II) ion, suggesting that a solvent screening effect takes place. Therefore it can be concluded that the counterions are far enough from the Cu(II) ions to be regarded as ion pairs.

Finally, the Cl−Cl rdfs highest peak positions in the various simulations are 18.78, 10.73, >22, 5.38, and 9.48 Å showing that as on average counterions remain separated from each other in the bulk solution.

3.7. Atom Site Solvation by Water: Distances OT−HW, O−HW, N2−HW, and NC−HW. In this section we report the first—not necessarily the highest—peak location for the interactions of the H atom in water (HW) with the following atom sites: hydroxyl O (OT), amide O (O), amide N (N2), and tertiary amine N in the EDA core (NC). These atoms are selected among other atom types because they bear the highest negative partial charges according to DFT charge distribution calculations.[26]

Table 4 shows that with the exception of the hydroxyl oxygen (OT), the dendrimer atoms do not have a significant number of water molecules in their closest vicinity. This is inferred by the height of the first peak, which is in most cases much lower than one, i.e., the atomic density found at the first peak location is much lower than the bulk atomic density. The H-bond length OT−HW seems to be unusually short so it may be indicative of inadequacies in the force field description of the OH group.

4. Conclusions

This work highlights the importance of water in Cu(II) stabilization during ionic complexation to dendrimers and suggests that amide oxygen atoms and possibly to a lesser extent hydroxyl O atoms are likely to be the preferred coordination sites in EDA core PAMAM −OH terminated dendrimers.

In low generation dendrimers, coordination to amide oxygen and water oxygen seems to be dominant whereas coordination to the tertiary amine nitrogen in EDA core is expected to be less frequently found. Time evolution of the distance between the ion and the tertiary amine N atoms indicates that their residence times are very short, suggesting a weaker coordination of Cu(II) to that site than that to the amide O and water O atoms.

The results from DFT calculations in dendrimer fragments, where branch folding effect is absent, can provide insights on how the Cu(II) ion coordinates in the outer pockets of large generation dendrimers. These calculations show cooperativity between the branching tertiary amine nitrogen, amide oxygen atoms, and water. However, as branch mobility and folding are expected to be higher in large generation dendrimers, the latter statement needs to be taken with caution

MD simulations incorporating the full solvent effect reveal that both "closed" configurations where the dendrimer branches contribute to a "cage" effect, and "open" structures may be found. In the gas phase, such closed configurations are found energetically favorable (by ∼6 kcal/mol) to the open ones. Moreover, closed configurations are also found in structures showing two-ion attachments to G0-OH, where a strong participation of the dendrimer branches in complexation is observed.

Analyses of the various complexation structures of Cu(II) in various degrees of hydration indicates that combined effects of shorter and stronger bonds, H-bonding enhanced stability, and chelate formation can explain why Cu(II) hexahydrates tend to lose some of their coordination waters to bind to the dendrimer sites.

Solvent screening effects can account for obtaining a Cu(II)/dendrimer load ratio of at least 2:1, which is expected to be maximum as the ionic separation is approximately equal to the dendrimer size with branches flatly extended. We did not observe ion pairing between Cu^{2+} and Cl^{-} but the results cannot be extended to larger generation dendrimers where the available area for counterion contact is larger.

Finally, this study expects to provide a motivation for fundamental experimental research related to low generation dendrimers as potential generators of useful insights that can help in explaining experimentally observed phenomena in dendrimers of larger generations; such valuable insights can be enhanced upon integration of theory and experiment.

Acknowledgment. This work is supported by National Science Foundation grant CTS-0103135. Supercomputer time granted by the National Energy Research Scientific Computing Center (NERSC) and by the DoD Major Shared Resource Centers (ARL MSRC and ASC MSRC) is gratefully acknowledged.

References and Notes

(1) El-Sayed, M.; Kian, M. F.; Naimark, M. D.; Hikal, A. H.; Ghandehari, H. *Pharm. Res.* **2001**, *18*, 23.

(2) Barron, J. A.; Bernhard, S.; Houston, P. L.; Abruna, H. D. *J. Phys. Chem. A* **2003**, *107*, 8130.

(3) Frechet, J. M. J. *J. Polym. Sci. Part A*: *Polym. Chem.* **2003**, *41*, 3713.

(4) Niu, Y.; Crooks, R. M. *C. R. Chimie* **2003**, *6*, 1049.

(5) Scott, R. W. J.; Wilson, O. M.; Crooks, R. M. *J. Phys. Chem. B* **2005**, *109*, 692.

(6) Zhao, M.; Crooks, R. M. *Adv. Mater.* **1999**, *11*, 217.

(7) Zhao, M.; Crooks, R. M. *Angew. Chem., Int. Ed.* **1999**, *38*, 364.

(8) Esumi, K.; Isono, R.; Yoshimura, T. *Langmuir* **2004**, *20*, 237.

(9) Esumi, K.; Susuki, A.; Yamahira, A.; Torigoe, K. *Langmuir* **2000**, *16*, 2604.

(10) Balogh, L.; Tomalia, D. *J. Am. Chem. Soc.* **1998**, *120*, 7355.

(11) Balogh, L.; Valluzzi, R.; Laverdure, K. S.; Gido, S. P.; Hagnauer, G. L.; Tomalia, D. A. *J. Nanopart. Res.* **1999**, *1*, 353.
(12) Crooks, R. M.; Lemon, B. I., III; Sun, L.; Yeung, L. K.; Zhao, M. *Top. Curr. Chem.* **2001**, *212*, 81.
(13) Diallo, M. S.; Balogh, L.; Shafagati, A.; Johnson, J. H.; Goddard, W. A.; Tomalia, D. A. *Environ. Sci., Technol.* **1999**, *33*, 820.
(14) Diallo, M. S.; Christie, S.; Swaminathan, P.; Balogh, L.; Shi, X.; Um, W.; Papelis, C.; Goddard, W. A.; Johnson, J. H., Jr. *Langmuir* **2004**, *20*, 2640.
(15) Balogh, L.; Tomalia, D. A.; Hagnauer, G. L. *Chem. Innovation* **2000**, *30*, 19.
(16) Ottaviani, M. F.; Montalti, F.; Turro, N. J.; Tomalia, D. A. *J. Phys. Chem. B* **1997**, *101*, 158.
(17) Tran, M. L.; Gahan, L. R.; Gentle, I. R. *J. Phys. Chem. B* **2004**, *108*, 20130.
(18) Ottaviani, M. F.; Bossmann, S.; Turro, N. J.; Tomalia, D. A. *J. Am. Chem. Soc.* **1994**, *116*, 661.
(19) Floriano, P. N.; Noble, C. O. I.; Schoonmaker, J. M.; Poliakoff, E. D.; McCarley, R. L. *J. Am. Chem. Soc.* **2001**, *123*, 10545.
(20) Scott, R. W. J.; Wilson, O. M.; Crooks, R. M. *J. Phys. Chem. B* **2005**, *109*, 692.
(21) Berendsen, H. J. C.; Grigera, J. R.; Straatsma, T. P. *J. Phys. Chem.* **1987**, *91*, 6269.
(22) Mayo, S. L.; Olafson, B. D.; Goddard, W. A. *J. Phys. Chem.* **1990**, *94*, 8897.
(23) Mulliken, R. S. *J. Chem. Phys.* **1955**, *23*, 1833.
(24) Mulliken, R. S. *J. Chem. Phys.* **1955**, *23*, 1841.
(25) Mulliken, R. S. *J. Chem. Phys.* **1955**, *23*, 2338.
(26) Tarazona-Vasquez, F.; Balbuena, P. B. *J. Phys. Chem. B* **2004**, *108*, 15982.
(27) Frisch, M. J.; Trucks, G. W.; Schlegel, H. B.; Scuseria, G. E.; Robb, M. A.; Cheeseman, J. R.; Montgomery, J. A., Jr.; Vreven, T.; Kudin, K. N.; Burant, J. C.; Millam, J. M.; Iyengar, S. S.; Tomasi, J.; Barone, V.; Mennucci, B.; Cossi, M.; Scalmani, G.; Rega, N.; Petersson, G. A.; Nakatsuji, H.; Hada, M.; Ehara, M.; Toyota, K.; Fukuda, R.; Hasegawa, J.; Ishida, M.; Nakajima, T.; Honda, Y.; Kitao, O.; Nakai, H.; Klene, M.; Li, X.; Knox, J. E.; Hratchian, H. P.; Cross, J. B.; Bakken, V.; Adamo, C.; Jaramillo, J.; Gomperts, R.; Stratmann, R. E.; Yazyev, O.; Austin, A. J.; Cammi, R.; Pomelli, C.; Ochterski, J. W.; Ayala, P. Y.; Morokuma, K.; Voth, G. A.; Salvador, P.; Dannenberg, J. J.; Zakrzewski, V. G.; Dapprich, S.; Daniels, A. D.; Strain, M. C.; Farkas, O.; Malick, D. K.; Rabuck, A. D.; Raghavachari, K.; Foresman, J. B.; Ortiz, J. V.; Cui, Q.; Baboul, A. G.; Clifford, S.; Cioslowski, J.; Stefanov, B. B.; Liu, G.; Liashenko, A.; Piskorz, P.; Komaromi, I.; Martin, R. L.; Fox, D. J.; Keith, T.; Al-Laham, M. A.; Peng, C. Y.; Nanayakkara, A.; Challacombe, M.; Gill, P. M. W.; Johnson, B.; Chen, W.; Wong, M. W.; Gonzalez, C.; Pople, J. A. *Gaussian 03*, Revision C.02; Gaussian, Inc., Wallingford CT, 2004.
(28) Rappe, A. K.; Goddard, W. A. *J. Phys. Chem.* **1991**, *95*, 3358.
(29) Rappe, A. K.; Casewit, C. J.; Colwell, K. S.; Goddard, W. A.; Skiff, W. M. *J. Am. Chem. Soc.* **1992**, *114*, 10024.
(30) Hay, P. J.; Wadt, W. R. *J. Chem. Phys.* **1985**, *82*, 270.
(31) Tarazona-Vasquez, F.; Balbuena, P. B. *J. Phys. Chem. B* **2004**, *108*, 15992.
(32) Mansfield, M. L.; Klushin, L. I. *Macromolecules* **1993**, *26*, 4262.
(33) Naidoo, K. J.; Hughes, S. J.; Moss, J. R. *Macromolecules* **1999**, *331*, 1.
(34) Smith, W.; Forester, T. R. *Comput. Phys. Commun.* **1994**, 52.
(35) Krol, M. *J. Mol. Model.* **2003**, *9*, 316.
(36) Lee, I.; Athey, B. D.; Wetzel, A. W.; Meixner, W.; Baker, J. R., Jr. *Macromolecules* **2002**, *35*, 4510.
(37) Streett, W. B.; Tildesley, D. J.; Saville, G. *Mol. Phys.* **1978**, 639.
(38) Hoover, W. *Phys. Rev. A* **1985**, *31*, 1695.
(39) Smith, W.; Forester, T. R. *DL_POLY*; Daresbury Laboratory: Daresbury, 1996.
(40) Car, R.; Parrinello, M. *Phys. Rev. Lett.* **1985**, *55*, 2471.
(41) Pasquarello, A.; Petri, I.; Salmon, P. S.; Parisel, O.; Car, R.; Toth, E.; Powell, D. H.; Fischer, H. E.; Helm, L.; Merbach, A. E. *Science* **2001**, *291*, 856.
(42) Schwenk, C. F.; Rode, B. M. *Chem. Phys. Chem.* **2003**, 931.
(43) Erras-Hanauer, H.; Clark, T.; Eldik, R. v. *Coord. Chem. Rev.* **2003**, *238*−*239*, 233.
(44) Marcus, Y. *Chem. Rev.* **1988**, *88*, 1475.
(45) Beagley, B.; Eriksson, A.; Lindgren, J.; Persson, I.; Pettersson, L. G. M.; Sandstrom, M.; Wahlgren, U.; White, E. W. *J. Phys. Condens. Matter* **1989**, *1*, 2395.
(46) Bopp, P.; Janscó, G.; Heinzinger, K. *Chem. Phys. Lett.* **1983**, *98*, 129.
(47) Helm, L.; Merbach, A. E. *Coord. Chem. Rev.* **1999**, *187*, 151.
(48) Bosman, A. W.; Schenning, A. P. H. J.; Janssen, R. A. J.; Meijer, E. W. *Chem. Ber./Recl.* **1997**, *130*, 725.
(49) D'Angelo, P.; Bottari, E.; Festa, M. R.; Nolting, H.-F.; Pavel, N. V. *J. Phys. Chem. B* **1998**, *102*, 3114.
(50) Choy, J.-H.; Kim, D.-K.; Park, J.-C.; Choi, S.-N.; Kim, Y.-J. *Inorg. Chem.* **1997**, *36*, 189.
(51) Persson, I.; Persson, P.; Sandstrom, M.; Ullstrom, A. S. *J. Chem. Soc., Faraday Trans.* **2002**, 1256.
(52) Ottaviani, M. F.; Valluzzi, R.; Balogh, L. *Macromolecules* **2002**, *35*, 5105.
(53) Tarazona-Vasquez, F.; Balbuena, P. B. Unpublished work.
(54) *Handbook of Chemistry and Physics*, 77th ed.; Lide, D. R., Ed.; CRC Press: Boca Raton, FL, 1997.
(55) Bromley, S. T.; Sankar, G.; Catlow, C. R. A.; Maschmeyer, T.; Johnson, B. F. G.; Thomas, J. M. *Chem. Phys. Lett.* **2001**, *340*, 524.
(56) Carrado, K. A.; Wasserman, S. R. *J. Am. Chem. Soc.* **1993**, *115*, 3394.
(57) Cox, C.; Wack, H.; Lectka, T. *Angew. Chem., Int. Ed.* **1999**, *38*, 798.
(58) Naylor, A. M.; Goddard, W. A.; Kiefer, G. E.; Tomalia, D. A. *J. Am. Chem. Soc.* **1989**, *111*, 2339.
(59) Scott, A. P.; Radom, L. *J. Phys. Chem.* **1996**, *100*, 16502.